Confinement of Polysoaps in Membrane Lyotropic Phases

Y. Yang and R. Prudhomme
Department of Chemical Engineering, Princeton University, Princeton, New Jersey 08544

K. M. McGrath
Chemistry Department, University of Otago, P.O. Box 56, Dunedin, New Zealand

P. Richetti and C. M. Marques
CNRS/Rhone-Poulenc, Complex Fluids Laboratory UMR166, Cranbury, New Jersey 08512-7500
(Received 11 November 1997)

We study the confinement of polysoaps in lyotropic smectic (L_α) and sponge (L_3) solutions of the nonionic surfactant pentaethylene glycol dodecyl ether ($C_{12}EO_5$). The polysoap is a hydrophobically modified polymer with *n*-tetradecyl sidegroups randomly grafted to a polyacrylate backbone. Without the hydrophobic side chains the backbone polymer cannot be embedded into the intermembrane space, but confinement is achieved for a polysoap with as low as 1% of grafted groups. We measure by small angle x-ray and neutron scattering an increase of the bending rigidity of the lamellar membranes as a function of polysoap concentration. [S0031-9007(98)05642-7]

PACS numbers: 83.70.Hq, 64.75.+g, 82.65.Dp

Fluid membranes are two-dimensional structures, self-assembled from surfactant solutions [1]. In the biological realm, phospholipid bilayers constitute the walls of liposomes and cells, hosting proteins responsible for functions as diverse as anchoring the cytoskeleton, providing coating protection against the body immune response or opening ionic channels for osmotic compensation [2]. Membranes are also present in many surfactant based industrial formulations. For instance, the processing and delivery of detergents or conditioning agents often require at some stage the use of concentrated surfactant solutions where lyotropic liquid crystals are formed [3]. The simplest liquid crystalline phase of membranes is the lamellar phase L_α, a smectic *A* lyotropic liquid crystal [4]. It consists of one-dimensional stacks of surfactant bilayers, separated by a solvent. Its one-dimensional symmetry allows for a relatively straightforward experimental determination of many properties pertaining not only to the ordered phase as a collective body of interacting membranes but also to each individual bilayer with its intrinsic constitutive elasticity [5]. Also of interest for our study is the sponge phase L_3, a bicontinuous isotropic phase of multiconnected membranes [6]. The wealth of information collected over the past two decades on L_α and L_3 phases designates them as convenient tools to investigate interactions between membranes and other components often present in synthetic or naturally occurring colloidal suspensions. L_α phases have for instance been used to host ferromagnetic colloidal particles [7] and different types of polymers [8–11], both in the intermembrane solvent subphase [12,13] and inside the bilayer itself [14]. In this Letter we investigate by small angle x-ray and neutron scattering the structure of L_α and L_3 phases with embedded polysoaps, a particular class of macromolecular surfactants. By studying a system of very flexible membranes, we were able to quantitatively determine, for the first time, the variation of the elastic constant of the membranes as a function of the concentration of added polymer.

The L_α and L_3 phases under investigation are composed of membranes of the nonionic surfactant $C_{12}EO_5$ (from Nikko, Japan) and hexanol in a NaCl brine solution at 0.1M. Pure water/$C_{12}EO_5$ mixtures have a wide L_α phase region at 60 °C, spanning membrane volume fractions ϕ from as low as $\phi = 0.005$ to ϕ of order unity [6]. For a perfectly flat array of ordered membranes of 2.5 nm thickness, this would correspond to interlamellar distances $d = 25/\phi$ nm in the range 0–250 nm. Adding hexanol to the membrane brings the wide lamellar range of the phase diagram to room temperature and reduces the membrane rigidity [5]. The surfactant/alcohol mole ratio in our samples is 1:1.43, which reduces the membrane rigidity to k_BT. Under these conditions the L_α phase is stable at 25 °C from $\phi = 0.04$ up to, at least, $\phi = 0.5$. The presence of salt in the solution effectively screens the electrostatic interactions of the added anionic polymers, the Debye length ℓ_D is, for the NaCl solution at 0.1M, of the size of a few monomers, $\ell_D \simeq 1.0$ nm. The polymers investigated in this work were prepared by grafting different densities of *n*-tetradecyl sidegroups to a backbone of poly(acrylic acid), PAA. Details of the reaction [15] and materials will be reported elsewhere [16]. In the brine solution, the hydrophobically modified PAA can for practical purposes be viewed as an almost neutral chain with an average number of 3472 backbone monomers. A fraction α of these backbone monomers is randomly attached to hydrophobic chains of 14 carbon atoms. Polymers with such macromolecular architecture are commonly known as polysoaps.

In the absence of grafted sidegroups the polymer spans an average dimension of the order of 40 nm. The polymer

cannot be successfully mixed within the lamellar or sponge phases even for membrane dilutions of the order of $\phi = 0.04$ corresponding to intermembrane subphase regions as thick as $d = 62.5$ nm. However, for a membrane volume fraction $\phi = 0.20$, a hydrophobic level α of the order of 1.7% is sufficient to successfully incorporate the polymer into the lamellar stack. We will report elsewhere the details of the complete phase diagrams for polysoap/membrane mixtures with polysoaps of different hydrophobic content. Hereafter, we concentrate on polysoaps with a substituted fraction $\alpha = 3\%$, in L_α and L_3 phases with membrane volume fraction $\phi = 0.2$. Figure 1 sketches the anticipated structure of the mixed system. The polymer is likely to be strongly anchored to the bilayers by the hydrophobic groups, exposure of each tetradecyl chain to the water environment having an associated cost of roughly $15k_BT$ [17]. There are on average 33 monomers between each anchored group, spanning a distance of 1.5 nm. The anchored polysoap can then be regarded as a two-dimensional chain composed of $N = 104$ loops or blobs with size $a = 1.5$ nm. Note that the polymer is anchored to a fluid membrane; the positions of the anchoring points along the membrane are therefore not determined by the anchoring process but can relax to its most probable distribution. The characteristic size R of a self-avoiding chain in two dimensions follows the relation $R = N^{3/4}a$, with N the polymerization index and a the monomer size. At low enough concentrations the polysoaps are therefore isolated fluffy patches of an average size $R = (104)^{3/4} \times 1.5 = 48.8$ nm. Above the overlap surface coverage $\Gamma^\star = MR^{-2}$ (M is the mass of the polysoap) different chains will interact. For our polysoaps $\Gamma^\star$ is of the order of 0.2 mg m^{-2}. This corresponds to a polymer concentration c in the water subphase $c = \Gamma^\star/(d - \delta) = 1.6$ wt %, with $d = 16$ nm and membrane thickness $\delta = 2.5$ nm. We were able to incorporate up to 4 wt % of polysoap in the L_α phase and up to 2 wt % of polysoap in the sponge phase. Larger polymer concentrations led to phase separation between a polymer poor L_α or L_3 phase and a polymer rich isotropic solution. We present below experimental data for polysoap concentrations in the range 0–4 wt %.

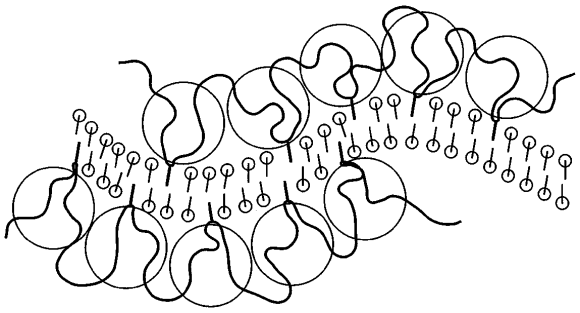

FIG. 1. Sketch of the string of blobs that the polymer forms when attaching to the membrane.

In a perfect one-dimensional stack of membranes, the intermembrane distance d is simply related to the membrane thickness δ and volume fraction ϕ by $d\phi = \delta$. However, flexible membranes fluctuate around their average position, leading to a smaller projected area and to an interlamellar distance which depends also on the membrane elastic constant k [18]

$$\frac{d\phi}{\delta} = 1 + \frac{1}{4\pi k} \ln\left[\frac{\delta}{\phi b} \sqrt{\frac{32k}{3\pi}} \right], \qquad (1)$$

where b is a microscopic cutoff length. The elastic constant is measured in units of k_BT. For flexible enough systems it is therefore possible to monitor changes of the elastic constant by simply measuring with x-ray or neutron scattering the variation of the interlamellar distance d.

Two-dimensional powder x-ray diffraction patterns of samples were obtained using a Rigaku (Tokyo, Japan) RU-200 rotating anode x-ray diffractometer equipped with a microfocus cup and a two-dimensional homebuilt Princeton photomultiplier area detector [19]. Small-angle neutron scattering experiments were performed at the Laboratoire Léon-Brillouin (CEN-Saclay, France) on the beam line PACE. In the samples for neutron scattering the water was replaced by D_2O, any other compound being the same.

We first determined the evolution of the interlamellar spacing d as a function of the membrane volume fraction ϕ, from the peak position q_0 of small-angle x-ray spectra, $d = 2\pi/q_0$. The best fit of the data with Eq. (1) gives a membrane thickness $\delta = 2.4 \pm 0.4$ nm and an elastic constant $k = 0.6 \pm 0.2$, if one fixes the value of the cutoff parameter at $b = 0.7$ nm. The values of the elastic constant and cutoff parameter are comparable to literature values for similar systems [5]. The value $b = 0.7$ nm for the cutoff parameter leads also to a good agreement between the membrane thickness δ obtained from the precedent fit, and the value of δ extracted from the high-q region of the neutron scattering spectra, shown in Fig. 2. The representation $q^4 I(q)$ was chosen to highlight the first oscillation from which we estimate a bilayer thickness $\delta = 2.4 \pm 0.2$ nm.

The neutron scattering data of the lamellar phase at fixed membrane volume fraction $\phi = 0.2$ is shown in Fig. 3 for different polymer concentrations. The data are shown after renormalizing the intensities $I(q)$ by their respective peak values $I(q_0)$ and the wave vectors q by the peak positions q_0. This representation emphasizes two important features of the scattering spectra. The first feature is the reduction of the peak width with increasing polymer concentration. This indicates a decrease of the exponent η that describes the power-law singularity [20,21] of the Bragg peak $I(q) \sim |q - q_0|^{-1+\eta}$. The exponent η is a function of the peak position q_0, the elastic constant of the bilayer k and $\bar{B}$, the compression modulus of the smectic phase: $\eta = q_0^2/(8\pi\sqrt{k\bar{B}/d})$ with k and

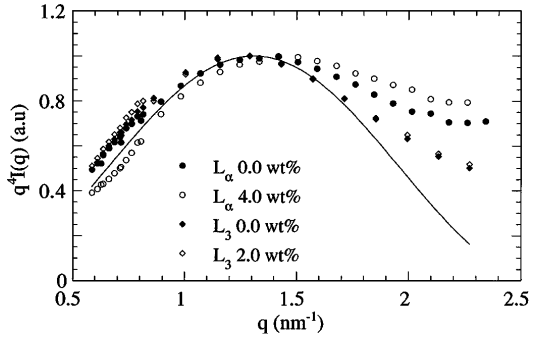

FIG. 2. Large-q behavior of $q^4 I_q$ in arbitrary units, showing one oscillation from which we extract the bilayer thickness $\delta = 2.4 \pm 0.2$ nm. The fitting line is the function $\sin^2(q\delta/2)$. We show data for the lamellar L_α phase without polymer and with 4% polymer, and for the sponge (L_3) phase without polymer and with 2% polymer.

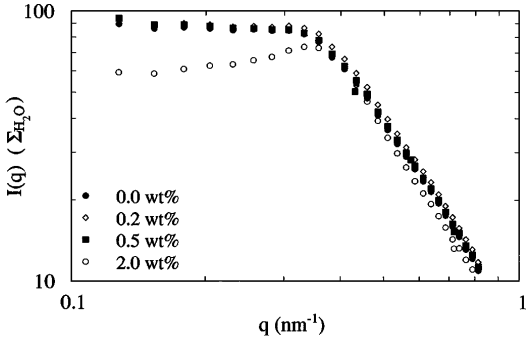

FIG. 4. Scattering data for the sponge phase at fixed membrane volume fraction $\phi = 0.2$ for different polymer concentrations as indicated.

$\bar{B}$ in units of $k_B T$. The observed reduction of the peak width corresponds therefore to an increase of the product $k\bar{B}$. The second feature is the variation of the intensity at small wave vectors $I(q \to 0)$. This intensity is related to the smectic modulus $\bar{B}$, $I(q \to 0) \simeq 1/\bar{B}$. A reduction of the intensity at low angles corresponds to an increase of $\bar{B}$ with polymer concentration. A larger smectic modulus $\bar{B}$ indicates a stiffening of the intermembrane interaction potential $V(d)$, $\bar{B} = d\partial^2 V/\partial d^2|_{d_{eq}}$. For a potential which is solely due to the steric Helfrich undulation interactions, the smectic modulus decreases with membrane stiffness $\bar{B} \sim 1/k$. However, as we will show below, k is also, in our case, an increasing function of polymer concentration: The undulation contribution to the modulus $\bar{B}$ should therefore decrease when polymer is added to the system. We conclude that the embedding of polymer in our system not only modifies the elastic properties of the membranes but also induces a new contribution $\Delta V(d)$ to the intermembrane potential $V(d)$. Further confirmation of the polymer induced stiffening of the surfactant bilayers is given by the evolution of the neutron scattering spectra of the sponge phase. This is shown in Fig. 4, where the reduction of the low angle intensity and the correspondent appearance of a correlation peak at intermediate wave vectors indicates an increase of the membrane elastic constant.

From the variation of the peak position q_0 in the scattering spectra of the lamellar phases, we extract the evolution of the interlamellar spacing $d = 2\pi/q_0$. Figure 5 shows the corresponding relative variation of the elastic constant k obtained, as explained above, by solving Eq. (1) for k at fixed ϕ and δ. The measured elastic constant k is an increasing function of polymer concentration. The contribution of the added polymer to the bilayer rigidity appears to increase linearly with polymer concentration at small concentrations, and to slightly level off to a maximum relative value of 1.8 at polymer concentrations above the expected two-dimensional overlap concentration $\Gamma^\star$. The large error bars in Fig. 5 are due to a large sensitivity of the k values with respect to variations in the membrane thickness δ. We discuss now the possible reasons for the observed stiffening of the membrane.

The modification of the membrane rigidity k has been theoretically studied in a number of cases where the membrane interacts with polymers. Adsorbed and nonadsorbed polymers are predicted [22,23] to reduce the elasticity of the membrane, while end-grafted polymers

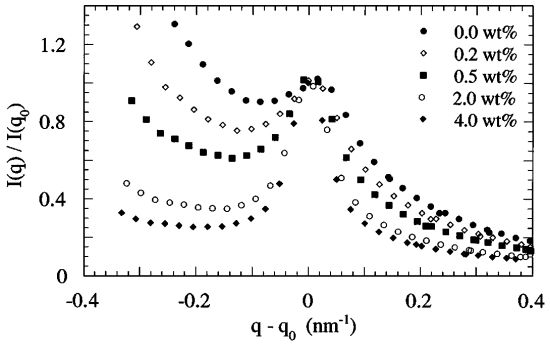

FIG. 3. Scattering data for the lamellar phase at fixed membrane volume fraction $\phi = 0.2$ and different polymer concentrations as indicated. The data have been normalized with respect to the positions and intensities of the peaks.

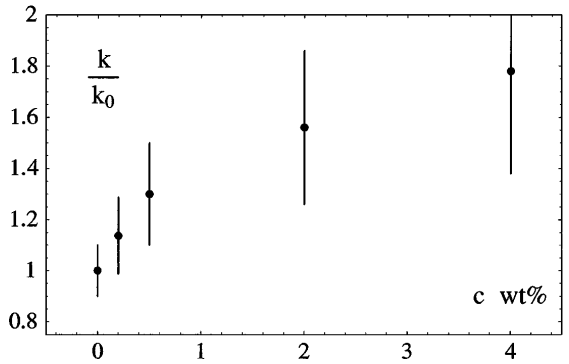

FIG. 5. Relative variation of the elastic constant $k(c)/k(c = 0)$ as a function of polymer concentration c.

are expected to increase k, both in the mushroom regime where the chains are sparsely grafted to the membrane [24–26] and in the brush regime where different chains interact strongly [27,28]. To our knowledge, the induced excess rigidity $\Delta k = k(c) - k(c = 0)$ has not been theoretically studied for a system of anchored polysoaps. For practical purposes the anchoring points provided by each of the side chains can be viewed as annealed grafting points, which remain attached to the membrane while freely exploring all allowed positions along the membrane. In the mushroom regime, it has been theoretically shown [24–26] that end-attached Gaussian polymers of index of polymerization P and monomer size a induce an excess rigidity $\Delta k = k_B T(\pi + 2)/12(\sigma_P R_P^2)$, with $R_P^2 = Pa^2$ the end-to-end radius of the polymer and σ_P the surface density of grafted polymers. For low surface densities σ of polysoaps, we estimate the induced membrane stiffening by simply adding the effect of each of the anchored half loops: $\Delta k = k_B T(\pi + 2)/12N\sigma R_P^2 = k_B T(\pi + 2)/12(\sigma R_{\text{gauss}}^2)$, if the anchored polysoaps obeyed Gaussian statistics with a radius $R_{\text{gauss}}^2 = NPa^2$. This gives an excess rigidity of roughly $0.4 k_B T$ at the overlap concentration $\sigma^\star = \Gamma^\star/M$. We expect the σR^2 scaling to also apply when excluded volume interactions are considered, albeit with a different prefactor. The observed elastic constant increase is therefore compatible with a polymer induced stiffening of the membrane.

Collective membrane effects can also translate into an effective increase of the observed k value. For instance, even in the absence of intrinsic rigidification, the grafted polymer layer translates into an effectively thicker membrane (this is not seen in the neutron scattering spectra for contrast reasons). This effect implies an additional factor in Eq. (1) of the form $1/(4\pi k)\ln(1 - a/d)$, which also leads to a reduction of the membrane interspacing. For our case where $a/d \sim 0.1$ this can be neglected, but could become a dominant factor for thicker layers. Another possibility of variation in k induced by intermembrane interactions is given by electrostatics effects. Although we strongly screened the electrostatic interactions, a residual effect might persist under the conditions of our experiment where both the Debye and the Gouy-Chapman length are very small. A theoretical estimation [29] of the excess elasticity is provided by $\Delta k = k_B T \ell_D/(\ell_B \pi)$, with ℓ_B the Bjerrum length ($\simeq 0.7$ nm in water). We get an electrostatic contribution $\Delta k \sim 0.25 k_B T$, smaller than the neutral polymer contribution. A better assessment of the electrostatic effects requires a systematic study of the induced rigidity as a function of salt content.

We thank Professor Sol Gruner for enabling us to use the small-angle x-ray scattering beam line in his laboratory at Princeton University, and Loic Auvray for his kind hospitality at the Laboratoire Léon-Brillouin. Enlightening discussions with Didier Roux are also gratefully acknowledged.

[1] S. Safran, *Statistical Thermodynamics of Surfaces, Interfaces and Membranes* (Addison-Wesley, Reading, MA, 1994).
[2] B. Alberts, *Molecular Biology of the Cell* (Garland, New York, 1994).
[3] J. van de Pas *et al.*, Colloids Surf. A **85**, 221 (1994).
[4] *Statistical Mechanics of Membranes and Surfaces*, edited by D. Nelson, T. Piran, and S. Weinberg (World Scientific, London, 1989).
[5] F. Freyssingeas, E. Nallet, and D. Roux, Langmuir **12**, 6028 (1996).
[6] R. Strey *et al.*, J. Chem. Soc. Faraday Trans. **86**, 2253 (1990).
[7] P. Fabre *et al.*, Phys. Rev. Lett. **64**, 539 (1990).
[8] H. Ringsdorf, J. Venzmer, and F. Winnik, Angew. Chem., Int. Ed. Engl. **30**, 315 (1991).
[9] H. Warriner *et al.*, Science **271**, 969 (1996).
[10] I. Iliopoulos and U. Olsson, J. Phys. Chem. **98**, 1500 (1994).
[11] B. Demé, M. Dubois, T. Zemb, and B. Cabane, J. Phys. Chem. **100**, 3828 (1996).
[12] C. Ligoure, G. Bouglet, G. Porte, and O. Diat, J. Phys. II (France) **7**, 473 (1997).
[13] M. Ficheux, A. Bellocq, and F. Nallet, J. Phys. II (France) **823**, 5 (1995).
[14] E. Z. Radlinska *et al.*, Phys. Rev. Lett. **74**, 4237 (1995).
[15] T. K. Wang, I. Iliopoulos, and R. Audebert, Pol. Bull. **20**, 577 (1988).
[16] Y. Yang *et al.* (to be published).
[17] T. Annable, R. Buscall, R. Ettelaie, and D. Whittlestone, J. Rheol. **37**, 695 (1993).
[18] D. Roux *et al.*, Europhys. Lett. **17**, 575 (1992).
[19] M. Tate, S. Gruner, and E. Eikenberry, Rev. Sci. Instrum. **68**, 47 (1997).
[20] A. Caille, C. R. Acad. Sci., Ser. B **274**, 891 (1972).
[21] C. R. Safinya, E. B. Sirota, D. Roux, and G. R. Smith, Phys. Rev. Lett. **62**, 1134 (1989).
[22] J. T. Brooks, C. M. Marques, and M. E. Cates, Europhys. Lett. **14**, 713 (1991).
[23] J. T. Brooks, C. M. Marques, and M. E. Cates, J. Phys. II (France) **6**, 673 (1991).
[24] C. Marques and J. Fournier, Europhys. Lett. **35**, 361 (1996).
[25] E. Eisenriegler, A. Hanke, and S. Dietrich, Phys. Rev. E **54**, 1134 (1996).
[26] R. Lipowsky, Europhys. Lett. **30**, 197 (1995).
[27] R. Cantor, Macromolecules **14**, 1186 (1981).
[28] S. T. Milner, T. A. Witten, and M. E. Cates, Macromolecules **22**, 853 (1989).
[29] J. Harden, C. Marques, J. Joanny, and D. Andelman, Langmuir **8**, 1170 (1992).